

Animal Coat Color and Radiative Heat Gain: A Re-Evaluation

G.E. Walsberg, G.S. Campbell, and J.R. King

Departments of Zoology, and Agronomy and Soils, Washington State University, Pullman, Washington 99164, USA

Accepted February 25, 1978

Summary. Thermal resistance and heat gain from simulated solar radiation were measured over a range of wind velocities in black and white pigeon plumages. Plumage thermal resistance averaged 39 % (feathers depressed) or 16 % (feathers erected) of that of an equivalent depth of still air. Feather erection increased plumage depth four-fold and increased plumage thermal resistance about 56 %. At low wind speeds, black plumages acquired much greater radiative heat loads than did white plumages. However, associated with the greater penetration of radiation into light than dark plumages, the radiative heating of white plumages is affected less by convective cooling than is that of black plumages. Thus, the heat loads of black and white plumages converge as wind speed is increased. This effect is most prominent in erected plumages, where at wind speeds greater than 3 m s^{-1} black plumages acquire lower radiative heat loads than do white plumages. These results suggest that animals with dark-colored coats may acquire lower heat loads under ecologically realistic conditions than those forms with light-colored coats. Thus, the dark coat colors of a number of desert species and the white coat color of polar forms may be thermally advantageous.

These results are used to test a new general model that accounts for effects of radiation penetration into a fur or feather coat upon an animal's heat budget. Even using simplifying assumptions, this model's predictions closely match measured values for plumages with feathers depressed (the typical state). Predictions using simplifying assumptions are less accurate for erected plumages. However, the model closely predicts empirical data for erected white plumages if one assumption is obviated by additional measurements. Data are not sufficient to judge whether this is also the case for erected black plumages.

List of Symbols

A	body surface area (m^2)
a_L	long-wave absorptivity of coat
a_s	short-wave absorptivity of coat
d	characteristic dimension (m)
E	evaporative water loss ($\text{kg m}^{-2} \text{s}^{-1}$)
h	coat thermal conductance ($\text{W m}^{-2} \text{°C}^{-1}$)
k	convection constant ($\text{s}^{\frac{1}{2}} \text{m}^{-1}$)
l	coat thickness (m)
L_i	long-wave irradiance at coat surface (W m^{-2})
M	metabolic heat production (W m^{-2})
m	body mass (kg)
P	plumage mass (kg)
p	probability per unit coat depth that a penetrating ray will strike a coat element (m^{-1})
$q(z)$	radiation absorbed at level z (W m^{-2})
R_{abs}	radiation absorbed by animal (W m^{-2})
r_e	external resistance to convective and radiative heat transfer (s m^{-1})
r_{Ha}	boundary layer resistance to convective heat transfer (s m^{-1})
r_{Hb}	whole-body thermal resistance (s m^{-1})
r_{Hc}	coat (plumage) thermal resistance (s m^{-1})
r_{Ht}	tissue thermal resistance (s m^{-1})
r_r	apparent resistance to radiative heat transfer (s m^{-1})
$r(z)$	thermal resistance from level z to coat surface (s m^{-1})
S_i	short-wave irradiance at coat surface (W m^{-2})
S^-	radiant flux going toward skin surface (W m^{-2})
S^+	radiant flux going away from skin surface (W m^{-2})
T_a	air temperature (°C)
T_b	core body temperature (°C)
T_e	equivalent black-body temperature (°C)
T_e'	air temperature plus temperature increment due to long-wave radiation (°C)
u	wind velocity (m s^{-1})
V	heat load on animal from short-wave radiation (W m^{-2})
z	depth within coat (m)
α	short-wave absorptivity of individual hairs or feather elements
ε	emissivity
η	$[(1 - \tau)^2 - \rho^2]^{\frac{1}{2}}$
λ	latent heat of vaporization of water (J kg^{-1})
ρ	short-wave reflectivity of individual hairs or feather elements
ρ^*	short-wave reflectivity of coat

ρ_s	short-wave reflectivity of skin
ρc_p	volumetric specific heat of air ($\text{J m}^{-3} \text{ }^\circ\text{C}^{-1}$)
σ	Stefan-Boltzmann constant ($\text{W m}^{-2} \text{ }^\circ\text{K}^{-4}$)
τ	short-wave transmissivity of individual hairs or feather elements
τ^*	short-wave transmissivity of coat

Introduction

The thermal significance of animal coat color and its ecological implications have been the subject of considerable discussion (e.g., Kovarik, 1964; Cowles, 1967; Hamilton and Heppner, 1967; Dawson and Brown, 1970; Hamilton, 1973). Though some analyses have suggested otherwise (e.g., Kovarik, 1964), it is generally assumed that animals with dark-colored coats, and hence greater absorptivity to short-wave radiation, acquire greater solar heat loads than do animals with light-colored coats. This assumption seems intuitively obvious and conforms with available data on radiative heat gain and coat color in small birds (Hamilton and Heppner, 1967; Lustick, 1969). However, these pioneering studies may be misleading, since they were conducted within a limited range of boundary layer conditions affecting heat exchange between the animal surface and environment; all measurements were made in metabolic chambers with essentially no forced convection. Hutchinson and Brown (1969) demonstrated that such forced convection, which is often a dominant mode of heat transfer in nature, may alter the radiative heating of dark and light coats to different degrees. These differences were attributed to the greater penetration of radiation into light than dark coats, as has been confirmed by Cena and Monteith (1975a). In this study, we first develop a general model that accounts for effects of radiation penetration and that should allow prediction of the radiative heat load on animals with coats of differing physical characteristics (e.g., color and thermal resistance) under various environmental conditions. We then compare the model's predictions to the radiative heat gain of black and white pigeon plumages measured over a range of wind velocities.

Theory

The energy budget equation for an animal with fur or feathers can be written as (Robinson et al., 1976; Campbell, 1977):

$$M - \lambda E = \rho c_p (T_b - T_e) / (r_{\text{Hb}} + r_e) \quad (1)$$

where M and E are rates of metabolic heat production and evaporation per unit animal surface area,

λ is the latent heat of vaporization of water (2430 J g^{-1}), ρc_p is the volumetric specific heat of air ($1200 \text{ J m}^{-3} \text{ }^\circ\text{C}^{-1}$), T_b is the animal body temperature, T_e is the equivalent black-body temperature, r_e is the external resistance to convective and radiative heat transfer, and r_{Hb} is the whole-body thermal resistance, equal to the sum of coat resistance (r_{Hc}) plus tissue resistance (r_{Ht}). The equivalent temperature represents air temperature (T_a) plus a temperature increment due to radiant flux:

$$T_e = T_a + (r_e / \rho c_p) (R_{\text{abs}} - \varepsilon \sigma T_a^4). \quad (2)$$

Here, ε is the animal surface emissivity, σ the Stefan-Boltzmann constant ($5.67 \times 10^{-8} \text{ W m}^{-2} \text{ }^\circ\text{K}^{-4}$), and R_{abs} the average radiant flux density absorbed by the animal. The external resistance is further defined as the parallel sum of an apparent radiative resistance (r_r) and a boundary-layer resistance to convective heat flow (r_{Ha}):

$$1/r_e = 1/r_r + 1/r_{\text{Ha}} \quad (3)$$

where

$$r_r = \rho c_p / 4\varepsilon \sigma T_a^3 \quad (4)$$

and

$$r_{\text{Ha}} = k(d/u)^{1/2}. \quad (5)$$

Here, d is the characteristic dimension of the animal, u is wind speed, and k is a constant equal to 307 for laminar flow when the units of d and u are meters and meters per second, respectively.

Equation (1) was derived assuming that all of the radiant energy incident on the animal is absorbed at the animal's surface. A recent analysis (Cena and Monteith, 1975a) indicates that this is not the case. Radiation may penetrate quite deeply into even dense coats, and the depth of penetration is a function of the color and density of the coat. In this analysis, we will account for the penetration of short-wave radiation into the coat, but will continue to assume that long-wave radiation is absorbed at the coat surface. An energy budget equation which explicitly shows short-wave radiation can be obtained by writing R_{abs} as $a_s S_i + a_L L_i$, where a_s and a_L are short- and long-wave absorptivities for the animal, and S_i and L_i are average short- and long-wave irradiances at the animal surface. We now redefine the equivalent temperature as the air temperature plus only that part of the radiation increment due to long-wave radiation:

$$T_e = T_a + r_e (a_L L_i - \varepsilon \sigma T_a^4) / \rho c_p \quad (6)$$

and include the short-wave term explicitly in the energy budget equation:

$$M - \lambda E + r_e a_s S_i / (r_{Hb} + r_e) = \rho c_p (T_b - T_e) / (r_{Hb} + r_e). \quad (7)$$

In equivalent electrical circuit terms (Robinson et al., 1976), a current source of strength $a_s S_i$ is located at the outer coat surface. The heat from that source is divided so that a fraction, $r_{Hb} / (r_e + r_{Hb})$, goes to the environment, and a fraction, $r_e / (r_e + r_{Hb})$, contributes to the heat load of the animal.

When radiation penetrates the animal coat, the heat load on the animal can be expressed by an equation similar to Equation (7), except that the radiation absorbed at each layer in the coat is multiplied by the resistance from the point of absorption to the external environment, and the product is summed over the entire coat. The radiant flux that is absorbed by the skin is added to this to give the total heat load on the animal from short-wave radiation:

$$V = \frac{r_{Hc} + r_e}{r_{Hb} + r_e} \tau^* (1 - \rho_s) S_i + \int_0^l \frac{r_e + r(z)}{r_e + r_{Hb}} q(z) dz. \quad (8)$$

Here, $q(z)$ represents the radiation absorbed at the level z , $r(z)$ is the thermal resistance from level z to the coat surface, τ^* is the transmissivity of the coat for short-wave radiation, ρ_s is the reflectivity of the skin, and r_{Hc} is the coat thermal resistance (Fig. 1). The first term in Equation (8) represents the radiation absorbed by the skin and the second term is the

amount of heat absorbed by the coat and conducted to the animal body.

Integration of Equation (8) requires knowledge of the functional relationships between $q(z)$, $r(z)$, and z . The radiant energy absorbed at depth z is the change in radiant flux density in going from z to $z + dz$. Cena and Monteith (1975a) divide the radiant flux into components going toward and away from the skin surface; S^- and S^+ , respectively. The change in flux density with depth is $dS/dz = dS^-/dz - dS^+/dz$, and is given by Equations (4) and (5) of Cena and Monteith (1975a). The function $q(z)$ can therefore be written as

$$q(z) = \alpha p (S^+ + S^-). \quad (9)$$

Cena and Monteith give the following expressions for S^+ and S^- :

$$S^- = S_i [(1 - \tau - \rho_s) \sinh \eta p z + \eta \cosh \eta p z] / C, \quad (10)$$

$$S^+ = S_i [(\rho - \rho_s + \tau \rho_s) \sinh \eta p z + \eta \rho_s \cosh \eta p z] / C \quad (11)$$

where

$$C = (1 - \tau - \rho_s) \sinh \eta p l + \eta \cosh \eta p l \quad (12)$$

and

$$\eta = [(1 - \tau)^2 - \rho^2]^{\frac{1}{2}}. \quad (13)$$

Here, α , ρ , and τ are the absorptivity, reflectivity, and transmissivity of the individual hairs or feather elements which make up the coat, p is the probability per unit depth of coat that a ray will strike a coat element, and l is coat thickness. The product $p dz$ is the cross-sectional area of coat elements in a layer dz projected on a plane perpendicular to the penetrating ray, and the product pl is the total projected area of coat elements on a plane perpendicular to the ray.

Various assumptions could be made about the variation of $r(z)$ with z . The simplest is that the variation is linear so that

$$r(z) = r_{Hc} (1 - z/l). \quad (14)$$

Combining Equations (8), (9), (10), (11), and (14), and performing the integration gives:

$$V = \frac{r_e a_s S_i}{r_{Hb} + r_e} + \frac{r_{Hc}}{r_{Hb} + r_e} \frac{\alpha S_i}{\eta^2 p l} [1 + \rho^* - \tau^* (1 + \rho_s)]. \quad (15)$$

The first term in Equation (15) is the heat load the animal would experience if all radiation were absorbed at the surface of the coat, as is assumed in Equation (1). The second term corrects for the increased heat load produced by radiation penetrating into the coat.

If we assume that the reflectivity and transmissivity of individual coat elements are equal, then α

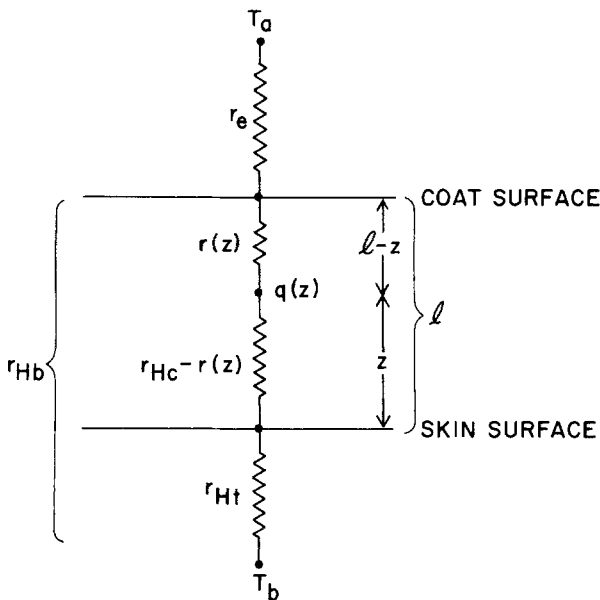


Fig. 1. Thermal resistances and depth variables used in determining the solar load due to penetration of the coat by short-wave radiation

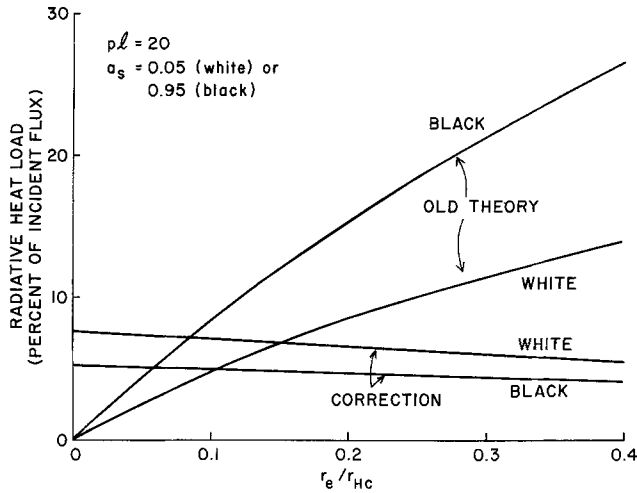


Fig. 2. Contributions of the first (old theory) and second (correction) terms of Equation (15) to fractional heat load as a function of the ratio of external to coat resistances. The actual heat load on an animal is the sum of the two terms

$=\eta^2$ and Equation (15) is specified entirely in terms of bulk coat properties. Figure 2 is plotted to show the magnitude of the two terms in Equation (15) using this assumption, a typical value of pl of 20 (Cena and Monteith, 1975a) and values of a_s typical of very white ($a_s=0.05$) and very black ($a_s=0.95$) coats. The fraction of incident solar radiation that contributes to body heat load is plotted as a function of the ratio r_e/r_{Hc} . For simplicity of presentation, it is assumed that r_{Hc} and r_{Hb} are equal; deviation from this assumption will produce identical relative changes in the first and second terms of Equation (15). When the external resistance is large (low windspeed or large characteristic dimension), the error resulting from the use of Equation (2) is small, but at small values of external resistance, errors using this assumption can be substantial. Note that it is possible under certain conditions to have higher heat loads on white coats than on black.

These equations predict that for small animals with fur or feathers, under outdoor conditions, the actual solar heat load may be about twice that predicted by the previous theory (Equation (2)) where it was assumed that all of the heat was absorbed at the coat surface (Fig. 2). The equivalent temperature equation (Equation (2)) can be corrected for this effect by adding the additional heat load to the short-wave term. The R_{abs} for Equation (2) then becomes

$$R_{abs} = a_L L_i + \{a_s + (r_{Hc}/r_e)(\alpha/\eta^2 pl)[1 + \rho^* - \tau^*(1 + \rho_s)]\} S_i. \quad (16)$$

Noting that $1 - \rho^* = a_s$ and assuming that $\rho = \tau$ and $\tau^*(1 + \rho_s) \ll 1 + \rho^*$ (though extent data are not suf-

ficient to evaluate the general validity of these assumptions), we finally obtain a form of this equation that may be adequate for most field studies

$$R_{abs} = a_L L_i + S_i [a_s + (r_{Hc}/r_e)(1/pl)(2 - a_s)]. \quad (17)$$

All of the parameters in this equation are easily measured or estimated, with the possible exception of pl . In the analysis so far, we have assumed that radiation penetrates the coat from only one angle. For diffuse radiation, coming from all angles, and for animals having surfaces with various orientations and inclinations to the radiant beam, it is probably reasonable to estimate, as Cena and Monteith (1975a) did, that the average value of p is around twice the value at normal incidence.

Bakken and Gates (1975) propose the use of metal casts of animals for field measurements of T_e , and suggest that these casts be either painted to duplicate the animal's absorptivity or covered by the animal's integument using taxidermy techniques. Our analysis indicates that for animals with fur or feather coats the latter alternative may be significantly more accurate, since simply painting the cast will underestimate the solar heat load by eliminating effects of radiation penetration.

Methods and Materials

A plumage preparation consisting of a section of skin and attached contour feathers in the form of a truncated triangle approximately 8 cm wide anteriorly, 15 cm long, and 15 cm wide posteriorly was removed from the breast and abdomen of 5 black and 5 white pigeons (*Columba livia*). Measurements were made using each plumage preparation with the feathers either maximally erected or maximally depressed. Initially, feathers were maximally erected on the fresh skin, which was then vacuum dried to maintain erection and eliminate effects of evaporation upon heat flux. After the measurements using erected plumages were completed, the skin was softened with distilled water, the feathers were maximally depressed, and the plumage again vacuum dried. A plumage preparation was mounted on the upper surface of a heat flux transducer/hot plate apparatus which was 8 cm wide anteriorly, 15 cm long, and 15 cm wide posteriorly (Fig. 3). Erected plumage depth was 3.0–3.2 cm over the heat flux transducer and depressed plumage depth was 0.7–0.9 cm. The skin surface was sealed to the upper plate surface with a thin layer of petroleum jelly. The temperature-controlled plate consisted of a sandwich of two 0.24 cm thick copper plates between which water at 40 °C (monitored with a thermocouple within the sandwich) was continuously circulated from a temperature-controlled reservoir. A 2.0 × 2.5 cm heat flux transducer (Tanner, 1963) was mounted in the center of the upper plate surface and surrounded by a 0.24 cm thick glass sheet which had a 0.013 cm thick aluminum sheet glued to the upper surface. These materials were of the same composition and thickness as that which made up the heat flux plate and, thus, the thermal resistance of the entire upper surface of the apparatus was essentially homogeneous. The lower surfaces of the heat flux transducer and the surrounding glass plate were sealed to the copper plate with heat sink compound. This entire unit was

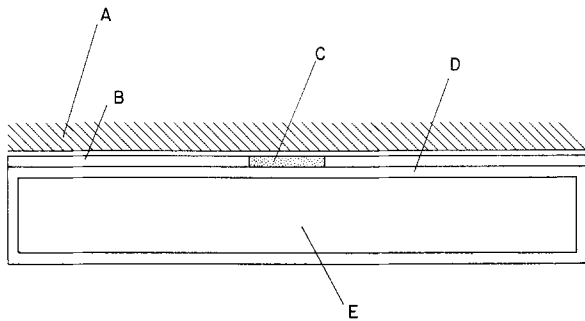


Fig. 3. Apparatus used in heat flux measurements. *A*, plumage preparation; *B*, glass plate; *C*, heat flux transducer; *D*, copper plate; *E*, interior chamber through which water at 40°C was circulated

calibrated by the method of Idso (1971). The resultant calibration factor differed only 5% from the sensitivity calculated using the thermal conductivity of the glass core and the number of thermocouple junctions in the heat flux plate (Fuchs and Hadas, 1973). The entire plumage/heat flux transducer/hot plate complex was placed into an environmental simulator so that the anterior end of the plumage preparation faced into the wind. For studies of erected feathers, an 8 cm wide wind shield was placed at a 45° angle at the anterior end of the apparatus. The upper edge of this shield extended to within 0.5 cm of the upper feather surface and greatly reduced depression of erected feathers by wind.

The thermal resistance of the feather coat (r_{fc}) was measured with the short-wave radiation source (xenon lamp, see beyond) and with a 10°C gradient across the plumage (plate temperature = 40°C, wall, roof, and air temperature = 30°C). Measurements were repeated under the same conditions with 900 W m⁻² of short-wave radiation on the upper plumage surface. Radiative heat gain was calculated as: (net heat flux with short-wave radiation) – (net heat flux without short-wave radiation). The external resistance to convective and radiative exchange from the plumage surface (r_e) was estimated by measuring heat flux from the bare heat flux transducer/hot plate complex with a 10°C temperature gradient between the plate (40°C) and the air, walls, and roof (30°C), and without short-wave radiation. An error in this estimate results from differences in surface temperature between the bare heat flux transducer/hot plate complex and the upper plumage surface. This affects the resistance to free convection, and the maximum error should occur when plumage surface temperatures are highest (i.e., in irradiated, depressed black plumages). The mean temperature of a thermocouple placed under a single feather vane on the upper surface of depressed black plumages at 0.25 m s⁻¹ was 79°C. Assuming that this equals the actual surface temperature and correcting for the 39°C temperature difference using Equation (6) of Robinson et al. (1976) reduces the estimated r_e only 9%. Thus, this maximum error is minor and surface temperature effects will be ignored.

Temperature gradients were measured vertically through erected plumages using a 0.2 cm diameter wooden dowel which had 11 0.01 cm diameter thermocouples mounted 0.3 cm apart and set at least 0.3 cm off the dowel. The dowel was inserted into the plumage at least 1.5 cm laterally from the nearest portion of the heat flux transducer. Because of their shallow depth, it was not possible to measure temperature gradients through depressed plumages.

Environmental Simulator

Measurements were made in an environmental simulator which allowed control of simulated solar radiation, the infrared environ-

ment (wall and roof temperatures), and air temperature and velocity (Hillman, 1974). This simulator consisted of a closed-system (recirculating) wind tunnel with a 30 cm deep, 39 cm high, 50 cm wide experimental chamber. Air entered through the anterior chamber wall, relative to the plumage orientation, and exited through the posterior wall. These walls consisted of aluminum tubes (painted flat black) for directing air flow. The remaining walls and the roof consisted of glass sandwiches through which fluid was circulated for temperature regulation.

Simulated Solar Radiation. Simulated solar radiation was provided by a 6000 W xenon lamp (Macbeth XBF 6000 W/l lamp). Though one of the best commercially available sources of simulated solar radiation (Grum, 1968), this lamp's spectrum differs from sunlight by being richer in the ultraviolet and having erratic peaks in the near-infrared. These differences were reduced by the filtration action of the roof sandwich, which consisted of two sheets of 0.5 cm pyrex glass, between which circulated a 1.0 cm thick layer of copper sulfate solution (8.5 g of CuSO₄ · 5 H₂O/liter of solution of 0.5% sulfuric acid in water). The pyrex glass reduced the ultraviolet energy and the CuSO₄ solution reduced the peaks in the near-infrared. Radiation intensity was measured with a Dirmhirn star pyranometer (Kahlsico #28AM100) and was maintained at 900 W m⁻². Reflectance from the chamber walls was minimized by painting them with Krylon ultra-flat black paint.

Infrared Environment. The lateral walls and the roof consisted of two plates of glass between which the copper sulfate solution was circulated from a temperature-controlled reservoir so that wall and roof temperatures were maintained at 30 ± 0.5°C. Temperatures were monitored with 0.01 cm diameter thermocouples glued to the inner glass surface. The wall thermocouples were painted flat black and the roof thermocouple was shielded from the xenon lamp by a small piece of aluminum foil. The aluminum tubes composing the anterior and posterior chamber walls through which air flowed were generally a few degrees warmer than the air due to irradiation from the xenon lamp.

Air Velocity. The environmental simulator formed a closed-circuit wind tunnel through which air was propelled by a blower powered by a variable speed motor. Air speed was measured 2 cm above the feather surface using an Alnor thermoanemometer which had been calibrated against a laboratory standard pitot tube.

Air Temperature. Air temperature was maintained at 30 ± 0.2°C and monitored with a thermocouple placed in the outflow of air from the experimental chamber. Temperature was regulated by circulating the air over a refrigerated coil which ran continuously and a heat coil which was controlled by a Honeywell W816B position-proportioning temperature controller in conjunction with a SSP140A resistance bulb sensor.

Reflectivity Measurements

Plumage reflectivity (ρ^*) was measured with a YSI Kettering model 65 radiometer fitted with a 0.1 cm thick quartz window. A 1.3 cm diameter, 7.5 cm long tube painted flat black was placed over the radiometer sensor and restricted the field of view to 10°. Measurements were made by placing the plumage preparation on the floor of the test chamber so that radiation from the xenon lamp was normal to the plumage surface and was reflected by the plumage at a 20° angle to the radiometer sensor. The quartz window on the sensor transmits equally all wavelengths in the 0.38–1.1 μm range produced by the xenon lamp after filtration. A plate with a 0.1 cm thick coat of Eastman white reflectance paint (BaSO₄ pigment, reflectivity = 0.99) was used as a standard by

Table 1. Plumage reflectivity and transmissivity^a

	Black		White	
	Depressed	Erected	Depressed	Erected
Reflectivity	0.14 ± 0.011	0.14 ± 0.015	0.83 ± 0.018	0.84 ± 0.020
Transmissivity	<0.001	<0.001	0.009 ± 0.0037	0.054 ± 0.018

^a Values are cited as $\bar{x} \pm \text{S.D.}$. Sample size in 5 in each case

placing it in the position and height of the feather surface. Reflectivity was calculated as the average of 10 measurements made of each plumage preparation.

Skin reflectivity (ρ_s) was not measured, but was assumed to equal 0.25 (Cena, 1966). Estimates of radiative heat gain are very insensitive to this assumption, since only a small fraction (0–5%) of incident radiation is transmitted to the skin.

Transmissivity Measurements

Plumage transmissivity (τ^*) was measured under a diffuse incandescent lamp using a sensitive blue-enhanced silicon cell mounted at the base of a 4.0 cm long, 16 ga. blunt hypodermic needle. A small hole was cut in the skin of the horizontally mounted plumage preparation and the needle was placed vertically beneath the skin so that its tip received radiation passing through the hole and the overlying plumage. Three measurements were made of each plumage preparation and transmissivity was calculated as the percentage of the radiation that impinged on the sensor with the plumage removed. The value of τ^* measured in this manner cannot be precisely reconciled with the ρ^* values measured with the Kettering radiometer, due to differences in lamp spectra and since the silicon cell is not equally responsive to all wavelengths. (The cell's sensitive range is 0.4–1.1 μm ; peak response occurs at 0.9 μm .) To the limited extent to which τ^* values are used in our analysis, however, this measurement probably is adequate.

Projected Feather Area per Unit Skin Surface

The projected area of feather elements per unit skin surface (pl) was calculated as the proportion of feather surface which is solid times the number of feather layers overlying the skin. This assumes that a particular feather's microscopic lattice is oriented at random with regard to that of feathers above and below it. This estimate also requires that feathers overlie each other in horizontal layers throughout the plumage depth, and thus pl was calculated only for depressed plumages. To estimate the proportion of the feather surface area which is solid, that is, excluding open space in the microscopic feather lattice, a contour feather was mounted on a glass slide and viewed at 440 power magnification. An ocular micrometer in the microscope projected a linear scale of 100 divisions into the field of view. The percent of the surface area which was solid was estimated by counting what percentage of the tips of the 100 dividing marks were projected onto solid structure. This was repeated 20 times at random areas and an average value calculated. The number of feather layers overlying the skin was estimated by weighing to the nearest 0.1 mg the mass of feathers removed by punching 3 0.64 cm holes through each depressed plumage preparation in the area that had been placed over the heat flux transducer. The standard weight for one 0.64 cm diameter circular section of feather was calculated as the average of 100 such sections punched through random areas of pigeon contour feathers. Data from all depressed plumages were lumped and a single average value was used in calculations. This average value was also assumed to apply to erected plumages.

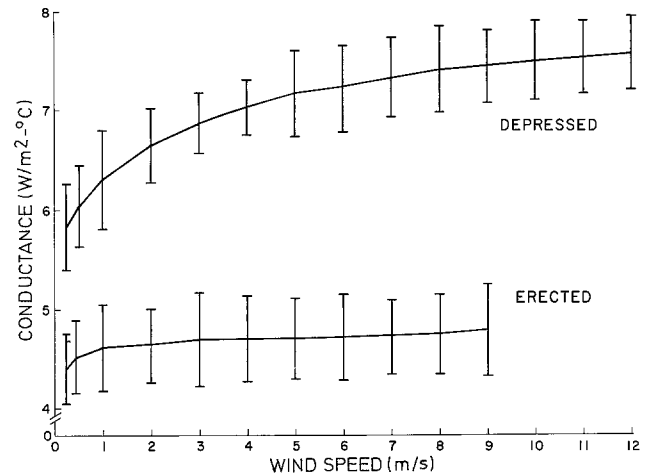


Fig. 4. Plumage conductance as a function of wind velocity. Values plotted are $\bar{x} \pm \text{S.D.}$; sample size is 10 in each case. Data for black and white plumages are combined since they did not differ significantly (Student's *t*-test, $P > 0.30$)

Results

General Physical Characteristics and Thermal Conductivity of Plumages

Plumage reflectivity and transmissivity are given in Table 1. Plumages consisted of 51 ± 5.41 ($\bar{x} \pm \text{S.D.}$) feather layers overlying the skin and solid structure represented $67 \pm 5.51\%$ ($\bar{x} \pm \text{S.D.}$) of feather surface area. Thus, the projected area of feather elements per unit skin surface (pl) averaged 34 for all plumages. (This value is a ratio of areas and is thus unitless.) Plumage conductance (h) as a function of wind velocity is shown in Figure 4. These values are converted to thermal resistances in Table 2 using the function $\rho c_p / h = r_{\text{total}} = r_e + r_{\text{Hc}}$. The resistance of the feather coat (r_{Hc}) was calculated by subtracting estimated values of r_e (Table 2). The estimated resistance of depressed plumages (0.7–0.9 cm deep) varies 6.3%, from 141 to 150 s m^{-1} ($\bar{x} = 147 \text{ s m}^{-1}$). This equals 39% of the value for a 0.8 cm layer of still air at 20 °C and is within the range of values for animal coats summarized by Monteith (1973). The estimated resistance of erected plumages (3.0–3.2 cm deep) varies 12%, from 211 to 236 s m^{-1} ($\bar{x} = 229 \text{ s m}^{-1}$). This

Table 2. Thermal resistances (s m^{-1})^a

Wind velocity (m s^{-1})	Depressed plumages			Erected plumages		
	r_{total}	r_e	r_{Hc}	r_{total}	r_e	r_{Hc}
0.25	206	65	141	273	62	211
0.50	199	55	144	265	50	215
1.0	190	42	148	260	39	221
2.0	180	31	149	258	30	228
3.0	175	25	150	255	25	230
4.0	171	22	149	255	22	233
5.0	167	20	147	255	19	236
6.0	166	18	148	254	18	236
7.0	164	17	147	253	16	237
8.0	162	16	146	252	15	237
9.0	161	15	146	250	14	236
10.0	160	14	146			
11.0	160	14	146			
12.0	158	13	145			

^a Values cited are means; sample size is 10 in each case

equals only 16% of the resistance of 3.0 cm of still air and is so low that substantial free convection and increased long-wave radiative heat transfer probably occur within the rather open structure of erected plumages (Cena and Monteith, 1975b).

Radiative Heat Gain

Figure 5 shows radiative heat gain through black and white plumages as a function of wind velocity. The heat gain of black plumages is much greater than that of white plumages at low wind velocities, thus confirming the results of Hamilton and Heppner (1967) and Lustick (1969), whose studies were conducted in essentially still air. However, the radiative heating of black plumages is much more wind-speed dependent than is that of white plumages, and the values for black and white plumages rapidly converge as wind speed increases. This effect is seen most prominently in erected plumages, in which white plumages acquire greater radiative heat loads than black plumages at wind velocities greater than 3 m s^{-1} . Above 5 m s^{-1} , erected black plumages acquire radiative heat loads lower than even depressed white plumages. The effect of ptiloerection upon radiative heat gain is qualitatively different for the two plumage colors—ptiloerection decreases the heat gain through black plumages but increases the heat gain through white plumages. At wind velocities greater than 4 m s^{-1} , the logarithm of radiative heat gain is essentially a linear function of air speed and least-squares regression lines fitted to the logarithmically transformed data allow extrapolation of measured values to flight speeds. Most birds fly at velo-

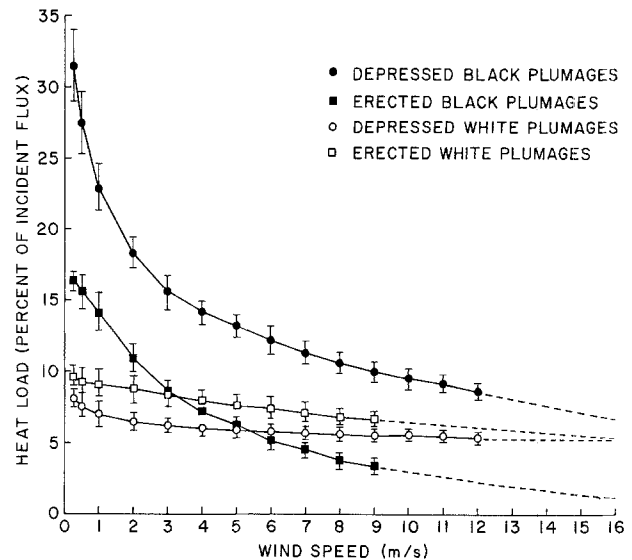


Fig. 5. Radiative heat gain as a function of wind velocity. Values plotted are $\bar{x} \pm \text{S.D.}$. Sample size is 5 in each case. Dashes show least-squares regression lines computed using data collected at wind speeds above 4 m s^{-1} . Equations for lines: $\log Y = -0.0265X + 1.25$ (depressed black plumages), $\log Y = -0.0642X + 1.12$ (erected black plumages), $\log Y = -0.00692X + 0.804$ (depressed white plumages), $\log Y = -0.0153X + 0.961$ (erected white plumages)

cities of 10 to 25 m s^{-1} ; the maximum range speed of *Columbia livia* is 16 m s^{-1} (Pennycuik, 1968, 1969). At 16 m s^{-1} , depressed black plumages should transmit a radiative heat load only slightly greater than that of white plumages (Fig. 5). In contrast to white plumages, feather erection in black plumages substantially reduces radiative heat gain, so that only a moderate degree of ptiloerection may produce heat loads equal to or below those that white plumages acquire.

Figure 6 compares the measured radiative heat gain of depressed plumages to that predicted using Equation (15) and assuming that $\alpha = \eta^2$. Theoretical predictions closely match the experimental results, with the greatest absolute difference occurring at $r_e = 65 \text{ s m}^{-1}$, when Equation (15) predicts a radiative heat load for black plumages of 29.4% of incident, which is 0.94 times the measured value of 31.3% of incident. The greatest proportional difference occurs in white plumages at $r_e = 13 \text{ s m}^{-1}$, when measured heat load (5.3% of incident) equals 0.84 times the value (6.3% of incident) predicted by Equation (15). Predictions essentially identical to those of Equation (15) would be made using the additional assumptions which were used in deriving Equation (17) from Equation (16), since only a small proportion (<1%) of incident radiation is transmitted to the skin. A much greater error would result if heat load in the experimental plumages were estimated using only the first term in Equation (15), which assumes that no

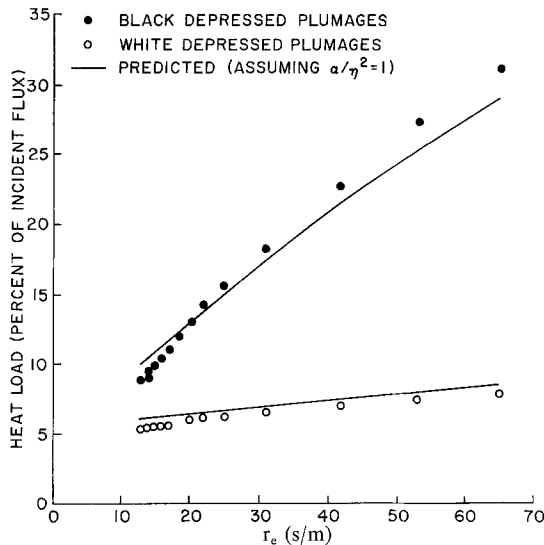


Fig. 6. Comparison of measured radiative heat gain in depressed plumages with that predicted using Equation (15) and assuming $\alpha/\eta^2 = 1$

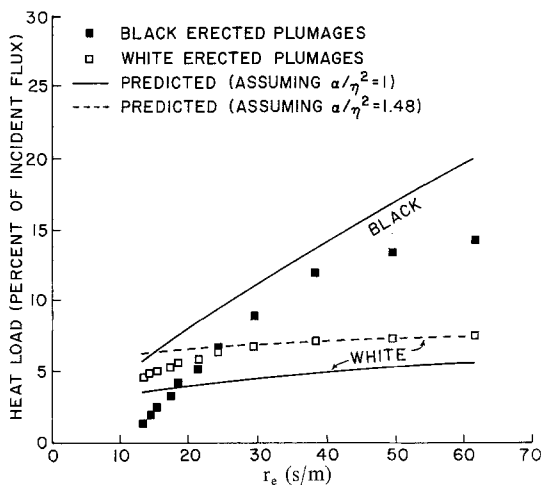


Fig. 7. Comparison of measured radiative heat gain in erected plumages with that predicted using Equation (15) and assuming either $\alpha/\eta^2 = 1.48$ (the calculated value for erected white plumages) or $\alpha/\eta^2 = 1$

radiation penetrates into the plumage. Compared to measured values, the first term in Equation (15) predicts radiative heat loads in depressed black plumages which are 13 to 19% too low (at $r_e = 65$ and 13 s m^{-1} , respectively). Errors would be greater in white plumages because of the greater radiation penetration, and heat load estimates using only the first term in Equation (15) are 37 to 75% too low (at $r_e = 65$ and 13 s m^{-1} , respectively).

Figure 7 compares measured radiative heat gain in erected plumages with that predicted using Equation (15). In white plumages, measured heat load is substantially higher than that predicted using the assumption $\alpha = \eta^2$. Indeed, radiative heat load in-

creased with feather erection in white plumages, while Equation (15) predicts that heat load should decrease if feather erection changes only the plumage thermal resistance. Apparently, the assumption that $\alpha = \eta^2$ becomes invalid in erected white plumages due to changes in the optical properties of the coat. Such changed optical properties are confirmed by the increased coat transmissivity observed after erection (Table 1). However, the ratio α/η^2 can be calculated directly in this case, since both coat reflectivity (ρ^*) and transmissivity (τ^*) were measured. Cena and Monteith (1975a) show that ρ^* is almost independent of ρ as long as the ratio α/ρ is constant. Since ρ^* changes only slightly with feather erection, the ratio α/ρ must be essentially constant. Equation (10) of Cena and Monteith (1975a) was used to find α/ρ by using an arbitrary value of ρ in the equation $\tau = 1 - \rho(1 + \alpha/\rho)$ to get τ and then varying α/ρ to obtain $\rho^* = 0.84$ (the experimental value). Since Equation (10) of Cena and Monteith (1975a) is essentially independent of the choice of ρ , any midrange value will produce the same value of α/ρ . Once the ratio α/ρ was known, Equation (12) of Cena and Monteith (1975a) was used to find ρ , to which the value of τ^* (which was measured) is quite sensitive. For erected white plumages, these calculations yield $\alpha/\rho = 0.015$, $\rho = 0.335$, $\tau = 0.668$, and $\alpha = 0.0049$. The ratio α/η^2 was calculated using these values and radiative heat load predicted using Equation (15) (Fig. 7). Here, theoretical predictions closely match measured values at high values of r_e , but deviate somewhat at low values of r_e . The maximum error occurs at $r_e = 13 \text{ s m}^{-1}$, when Equation (15) predicts a radiative heat load of 8.4% of incident, which is 1.25 times the measured value of 6.7%. Direct estimates of the ratio α/η^2 could not be obtained for erected black plumages because τ^* was immeasurably small. However, the heat load is predicted fairly well by Equation (15) if it is assumed that $\alpha = \eta^2$. It is possible that the lower than predicted heat load in black plumages is due to change in the α/η^2 ratio, but heat load is probably also reduced by free convection in the upper feather layers reducing the thermal resistance between the upper surface and the point of radiation absorption within the plumage ($r(z)$ in Fig. 1). Such free convection is most likely to be significant in erected black plumages, due to the rather open plumage structure and the steep temperature gradient produced in the upper feather layers by irradiation (Fig. 8).

Temperature Profiles Through Erected Plumages

Temperature profiles measured in erected plumages graphically illustrate how the interaction of convec-

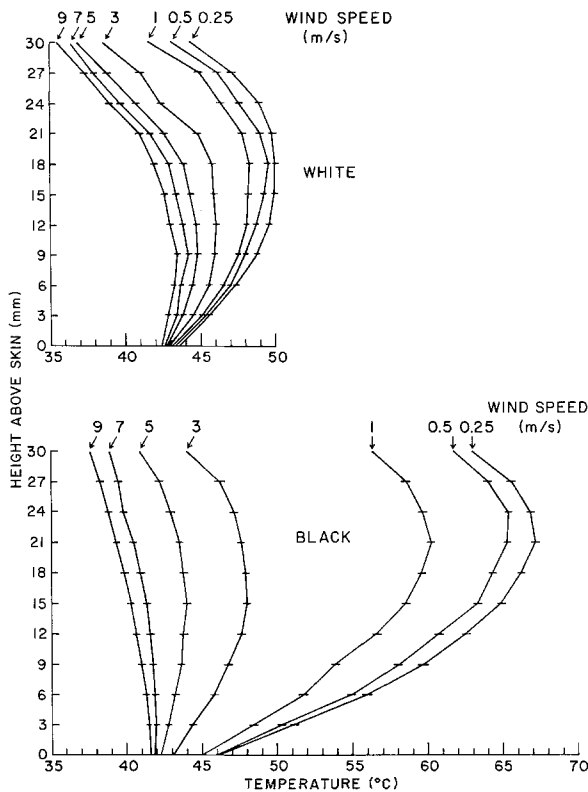


Fig. 8. Temperature profiles measured in erected plumages when irradiated. Values plotted are means and sample size is 5 in each case

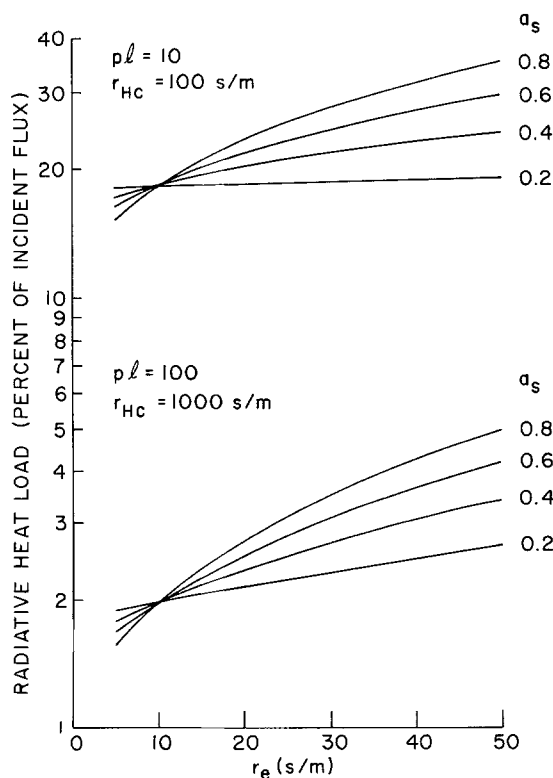


Fig. 9. Effect of differing coat depths upon radiative heat gain, assuming a constant pl/r_{Hc} ratio

itive cooling with the differential penetration of radiation into black and white plumages results in darker plumages acquiring a lower radiative heat load at all but the lowest wind speeds (Fig. 8). Because of their greater absorptivity, black plumages reach higher temperatures at low wind speeds than do white plumages. However, the highest temperatures in black plumages occur in a narrow band which peaks near the upper plumage surface. Temperatures in white plumages peak in a broad band midway through the plumage depth, which reflects the greater penetration of radiation through non-pigmented feathers. Since most radiation is absorbed near the upper surface of black plumages, the heating of these plumages is greatly reduced by increased forced convection. In contrast, the heat generated by irradiation in white plumages is insulated from forced convection by a greater depth of plumage. Thus, at 3 m s^{-1} wind the skin surface temperature and radiative heat gain beneath black plumages is virtually equal to that beneath white plumages. At higher wind speeds, skin surface temperature and radiative heat gain are lower in black plumages than in white plumages.

Discussion

Predictions from the Model:

Effects of Various Coat Characteristics and Body Sizes

Coat Depth and Body Size

Assuming a linear relation between feather mass and coat resistance, plumages composed of structurally similar feathers should exhibit a linear relation between feather area per unit skin surface (pl) and coat resistance (r_{Hc}). If this is so, pl is inversely related to radiative heat gain (Fig. 9). At higher values of pl (e.g., larger coat depth), the absolute difference in radiative heat gain between plumages of differing absorptivities is smaller, but the proportional differences remain the same. The value of r_e below which lighter plumages acquire greater heat loads than dark plumages is constant.

Smaller birds should generally have thinner coats and lower values of pl . Calder and King (1974) have shown that $P/A \propto m^{0.33}$, where P is plumage mass, A is body surface area, and m is body mass. Assuming a linear relation between pl and feather mass per unit skin surface, then $pl \propto m^{0.33}$. For example, in Figure 9, the value $pl=100$ would be expected to correspond with a body mass 1000 times greater than the value $pl=10$. Thus, at the same value of r_e , smaller birds will generally acquire greater radiative heat loads with greater absolute differences between plumages of different absorptivities.

Coat Thermal Resistance

If no other physical characteristics vary, radiative heat gain is constant for any particular value of the ratio r_e/r_{Hc} . Thus, changes in the coat resistance will shift the curve of radiative heat gain versus r_e in proportion to the change in r_{Hc} . The value of r_e below which lighter coats acquire a greater radiative heat load than darker coats will also shift directly in proportion to the change in r_{Hc} . Thus, a coat with a resistance twice that of another coat in which all other physical characteristics are similar will exhibit a crossover point at an r_e value twice as high (e.g., lower wind speeds).

Energetics and the Ecology of Plumage Coloration

To illustrate the potential ecological significance of the phenomena described in this study, the thermal behavior of the experimental black and white pigeon plumages can be estimated for extreme environmental conditions. In general, changes in the body to air temperature gradient will shift the heat flux of erected plumages relative to that of depressed plumages, due to the decreased thermal conductance induced by ptiloerection. Varying the intensity of incident solar radiation changes the absolute heat flux, but does not affect proportional differences in radiative heat gain between plumages of different absorptivities or degrees of feather erection. These projections are somewhat speculative, however, since differing air temperatures and levels of incident radiation will affect the resistances to heat loss by radiation and free convection from the coat surface. Thus, these estimates are only as valid as the assumption that forced convection is the dominant mode of heat transfer, which is probably true in small to medium sized animals above low wind speeds. It must be emphasized that these projections describe the estimated thermal behavior of the experimental plumage preparations and are not directly applicable to whole animals. For instance, the radiative heat loads are those of plumages perpendicular to the solar beam, as may occur on a bird's dorsal surface, and the heat load over the entire body surface may differ considerably. Irradiance would be lower when averaged over the entire body, since only a fraction of the total surface area is exposed to direct solar radiation. In addition, coat characteristics often vary greatly over an animal's surface, as exemplified by a number of bird species which while nesting often exhibit a white depressed plumage ventrally and a dark erected plumage dorsally (Naik et al., 1961; Howell and Bartholomew, 1962; Maclean, 1967; Grant and Hogg, 1976).

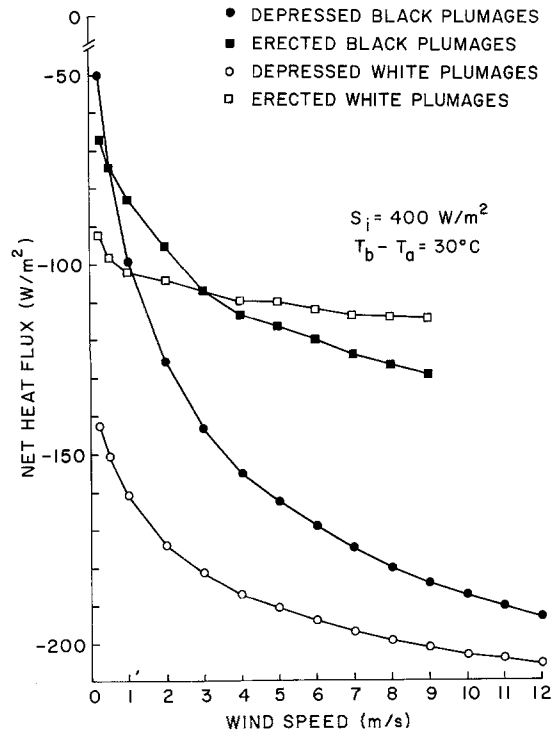


Fig. 10. Projected thermal behavior of the experimental plumages under winter conditions. Negative heat flux values indicate a net body heat loss

Figure 10 shows the estimated thermal behavior of the experimental pigeon plumages under a low radiation load (400 W m^{-2}) and at a low ambient temperature (30°C below body temperature). This estimate shows that at wind speeds greater than 3 m s^{-1} , conditions under which an animal is likely to be maximally cold-stressed, erected white plumages exhibit the lowest net heat loss, due to their greater thermal resistance and radiative heat gain. Thus, the white coats typical of polar homeotherms may be thermally the most advantageous. However, though these animals may benefit from this effect, it is likely that requirements for concealment against a snowy background have been a more important selective pressure than associated energetic advantages.

Figure 11 shows the estimated thermal behavior of the experimental plumages under extreme desert conditions—a high radiation load (1000 W m^{-2}) and an ambient temperature 10°C above body temperature. These results show that at all but the lowest wind speeds erected black plumages transmit the lowest net heat load to the skin, due to their high thermal resistance and low radiative heat gain. While ptiloerection has only a slight effect upon heat flux in white plumages, it has a strong effect in black plumages and it is possible that at flight speeds only a moderate degree of feather erection is required to reduce heat gain through black plumages to a level

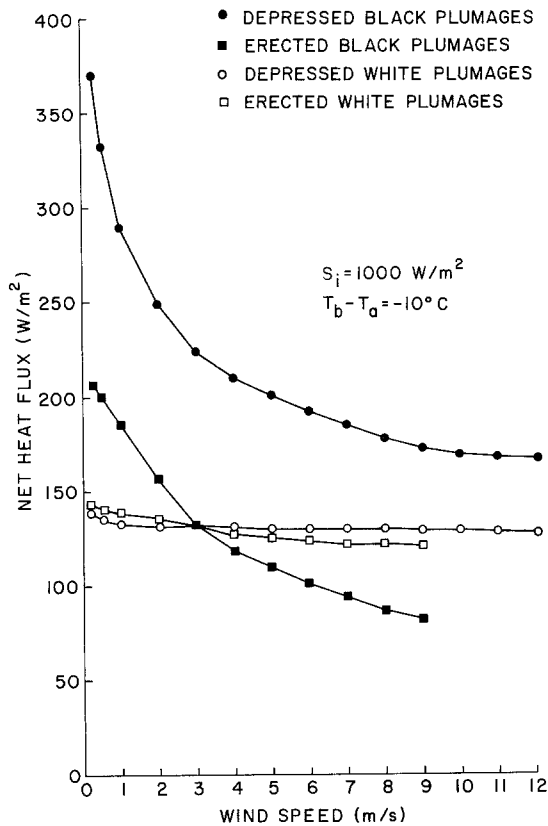


Fig. 11. Projected thermal behavior of the experimental plumages under extreme desert conditions. Positive heat flux values indicate a net body heat gain

equal to or below that of white plumages. These results offer a partial explanation for the apparent paradox noted by a number of authors (e.g., Buxton, 1923; Meinertzhagen, 1954) that black animals are the most common exceptions to the rule that desert animals are cryptically colored. Of course, the fact that some black desert birds may benefit from a decreased radiative heat gain does not mean that thermoregulation has been the sole, or even the most important, selective pressure operating on the evolution of their plumage coloration. In open habitats such as deserts, grasslands, and marshes, visual conspicuousness may be a more effective social signal over long distances than vocalizations. Black coloration produces maximum contrast against the sky and a black bird is often much more conspicuous than more brightly colored forms (Walsberg, 1977). Thus, it is not surprising that many territorial or flocking birds occupying open habitats are completely or partially black, such as many vultures, icterids, and corvids. There are desert species, however, in which control of solar heat gain appears to have been of primary importance in the evolution of dark plumages. Examples are seen in various gulls (*Larus* spp.). Gulls typically have white bodies with

light gray backs, but a few species are primarily dark gray over most of their body. The darkest gulls all nest in tropical or subtropical mainland deserts or desert islands. The only carefully studied species is the Gray Gull, *Larus modestus*, which nests during the summer in the Atacama Desert of Chile (Howell et al., 1974). In this gull's colonies, air temperatures typically range from 2 to 38 °C daily and ground surface temperatures near the nest, which consists simply of a shallow scrape in the soil, often exceed 50 °C, the upper limit of the instruments used by Howell and his co-workers. Though not measured, solar radiation is undoubtedly intense, due to the absence of shade usable to the gulls, the tropical latitude (about 22°S), the high altitude (1800 m), and the extremely dry and cloudless atmosphere. The incubating birds cannot escape these conditions even momentarily throughout the 14 h daylight period, since nest-relief occurs only at night and the eggs would reach lethal temperatures if exposed to the intense insolation. Apparently, the Gray Gull adapts to these conditions by matching the daily wind cycle with a daily pattern of ptiloerection. The plumage is maximally depressed during the calm mornings, but is maximally erected from early afternoon until night-fall, when there occurs invariably a strong (up to 9 m s⁻¹) and continuous wind. The thermal behavior of dark and light plumages presented in Figures 10 and 11 confirms the suggestion by Howell and his coworkers that this species' dark, depressed plumage during the windless, cold mornings should minimize cold stress and its dark, fully erected plumage during the windy, hot afternoon should minimize heat stress. Since factors such as concealment do not seem to have been important (there is virtually no predation in the nesting area), it is likely that thermoregulation was a major factor in the evolution of this desert species' dark coloration.

This investigation was supported by grants from the National Science Foundation (BMS 75-20338) and the National Institutes of Health (GM 01276).

References

- Bakken, G.S., Gates, D.M.: Heat transfer analysis of animals: some implications for field ecology, physiology, and evolution. In: Perspectives in biophysical ecology (eds. D.M. Gates, R.B. Schmerl), pp. 255–290. Berlin-Heidelberg-New York: Springer 1975
- Buxton, P.A.: Animal life in deserts. London: Edward Arnold and Co. 1923
- Calder, W.A., King, J.R.: Thermal and caloric relations of birds. In: Avian biology, Vol. 4 (eds. D.S. Farner, J.R. King), pp. 259–413. New York: Academic Press 1974
- Campbell, G.S.: An introduction to environmental biophysics. Berlin-Heidelberg-New York: Springer 1977
- Cena, K.: Absorption of solar radiation by cattle and horses with various coat colors. Acta Agr. Silv. 6, 93–138 (1966)

- Cena, K., Monteith, J.L.: Transfer processes in animal coats. I. Radiative transfer. *Proc. roy. Soc. Lond. B* **188**, 377–394 (1975a)
- Cena, K., Monteith, J.L.: Transfer processes in animal coats. II. Conduction and convection. *Proc. roy. Soc. Lond. B* **188**, 395–411 (1975b)
- Cowles, R.B.: Black pigmentation: Adaptation for concealment or heat conservation? *Science* **158**, 1340–1341 (1967)
- Dawson, T.J., Brown, G.D.: A comparison of the insulative and reflective properties of the fur of desert kangaroos. *Comp. Biochem. Physiol.* **37**, 23–38 (1970)
- Fuchs, M., Hadas, A.: Analysis of the performance of an improved soil heat flux transducer. *Soil Sci. Soc. Am. Proc.* **37**, 173–175 (1973)
- Grant, G.S., Hogg, N.: Behavior of late-nesting Black Skimmers at Salton Sea, California. *Western Birds* **7**, 73–80 (1976)
- Grum, F.: Artificial light sources for simulating natural daylight and skylight. *Appl. Opt.* **7**, 183–187 (1968)
- Hamilton, W.J., III: *Life's color code*. New York: McGraw-Hill 1973
- Hamilton, W.J., III, Heppner, F.: Radiant solar energy and the function of black homeotherm pigmentation: an hypothesis. *Science* **155**, 196–197 (1967)
- Hillman, P.E.: Simulation and modeling of transient thermal responses of the western fence lizard, *Sceloporus occidentalis*. Ph.D. Dissertation, Washington State University (1974)
- Howell, T.R., Araya, B., Millie, W.R.: Breeding biology of the Gray Gull, *Larus modestus*. *Univ. Calif. Publ. Zool.* **104**, 1–57 (1974)
- Howell, T.R., Bartholomew, G.A.: Temperature regulation in the Sooty Tern *Sterna fuscata*. *Ibis* **104**, 98–105 (1962)
- Hutchinson, J.C.D., Brown, G.B.: Penetrance of cattle coats by radiation. *J. appl. Physiol.* **26**, 454–464 (1969)
- Idso, S.B.: A simple technique for the calibration of long-wave radiation probes. *Agr. Meteorol.* **8**, 235–243 (1971)
- Kovarik, M.: Flow of heat in an irradiated protective cover. *Nature* **201**, 1085–1087 (1964)
- Lustick, S.: Bird energetics: effects of artificial radiation. *Science* **163**, 387–390 (1969)
- Maclean, G.L.: The breeding biology and behavior of the Double-banded Courser *Rhinoptilus africanus* (Temminck). *Ibis* **109**, 556–569 (1967)
- Meinertzhagen, R.: *Birds of Arabia*. Edinburgh: Oliver and Boyd 1954
- Monteith, J.L.: *Principles of environmental physics*. New York: American Elsevier Publ. Co. 1973
- Naik, R.M., George, P.V., Dixit, D.B.: Some observations on the behavior of the incubating Red-wattled Lapwing, *Vanellus indicus* (Bodd.). *J. Bombay Nat. Soc.* **58**, 223–230 (1961)
- Pennycuick, C.J.: Power requirements for horizontal flight in the pigeon, *Columba livia*. *J. exp. Biol.* **49**, 527–555 (1968)
- Pennycuick, C.J.: The mechanics of bird migration. *Ibis* **111**, 525–556 (1969)
- Robinson, D.E., Campbell, G.S., King, J.R.: An evaluation of heat exchange in small birds. *J. comp. Physiol.* **105**, 153–166 (1976)
- Tanner, C.B.: Basic instrumentation and measurements for plant environment and micrometeorology. *Univ. Wisconsin, Dept. Soils Sci. Bull.* **6**, S 1–15 (1963)
- Walsberg, G.E.: Ecology and energetics of contrasting social systems in *Phainopepla nitens* (Aves: Ptilonotidae). *Univ. Calif. Publ. Zool.* **108**, 1–63 (1977)